# Balancing a cylinder on a thin vertical layer of viscous fluid

J. Eggers,[1] R. R. Kerswell,[1] and T. Mullin[2]
[1] *School of Mathematics, University of Bristol, University Walk, Bristol BS8 1TW, United Kingdom*
[2] *Manchester Centre for Nonlinear Dynamics, The University of Manchester, Manchester M13 9PL, United Kingdom*
(Received 1 May 2013; published 25 June 2013)

We analyze recent experiments that show that a cylinder can be suspended in a stable position by placing it on a vertically moving belt that is covered by a thin layer of very viscous oil. The weight of the cylinder is supported by viscous forces in the fluid layer, and the cylinder rotates with respect to its axis in the direction of the belt motion. We propose a simple model for stable suspension of the cylinder, based on lubrication ideas.

DOI: 10.1103/PhysRevE.87.065001 PACS number(s): 47.15.gm, 47.85.mf

*Introduction.* The experiment we propose to analyze is shown schematically in Fig. 1. A smooth, steel reinforced polyurethane engine belt (375 mm long and 26.5 mm wide) is driven by a pair of 38-mm toothed pulleys that were matched to the teeth on the inside of the belt. The rotation rate of the drive was monitored using an optical shaft encoder to produce a belt speed $U_w$. The lower part of the belt turns inside a bath of silicone oil of density $\rho = 970 \pm 10$ kg/m$^{-3}$, kinematic viscosity $\mu/\rho = 13{,}740 \pm 140$ cSt, and surface tension $\gamma = 21.5$ mNm$^{-1}$. A constant film thickness $h$ between 0.1 and 1 mm is maintained by adjusting a scraper as the belt leaves the pool; viscous draining is found not to be significant. Our setup could serve as a model problem for the interaction between solids through a liquid film, as it arises, for example, in coating flows [1,2].

Cylinders of radii $R$ between 4 and 16 mm and variable density were brought into contact with the liquid layer and were found to remain stuck to the layer. Cylinders remained in an orientation perpendicular to the belt motion and were found to move up and down the belt at a constant speed. Repeating the same experiment many times, it was found that up to small fluctuations, cylinders established themselves at a given speed $U_r$ *relative* to the belt speed. This speed could be measured either by tracking the cylinder's motion or by adjusting the belt speed until the cylinder remained at a fixed height.

At the same time, the cylinder's angular frequency was measured; typically, slip velocities between the belt and the cylinder were between 0.3 and 0.65 $U_r$. It was found that results were *independent* of the length of the cylinder, indicating that the flow phenomenon is essentially two-dimensional. Experiments similar to ours were performed in Ref. [3], using spheres instead of cylinders; attempts with cylinders lead to a three-dimensional, unsteady, zigzag motion [3]. Since no data were reported, we can only speculate that this was because experiments were performed in a different parameter regime. At least for a vertical belt, or when up to 12° from the vertical, we always observed steady motion. Downstream of the cylinder (i.e., above it), we noticed the classical printer's instability [4], but this did not appear to have a significant effect on the motion of the cylinder.

Since inertial effects are small, this means that a steady state is specified completely by the fluid properties $\mu, \gamma$, geometrical parameters $h, R$, the weight $Mg$ of the cylinder per unit length, and the corresponding weight $\rho h R$ of the fluid column per unit length. Assuming that the weight of the fluid is inconsequential

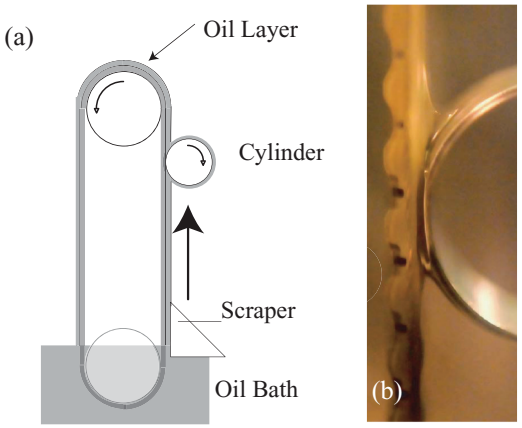


FIG. 1. (Color online) (a) Schematic diagram of the apparatus; (b) a side view of a hollow Aluminum cylinder (radius 4 mm) on the upward-moving vertical belt showing the converging belt and cylinder fluid layers upstream (below the cylinder) and diverging downstream (above the cylinder).

compared to that of the cylinder ($\rho h R/M \ll 1$), the two remaining dimensionless control parameters are [3]

$$\mathrm{Bo} = \frac{Mg}{\gamma}, \quad h_R = \frac{h}{R}. \tag{1}$$

In a laboratory frame of reference, in which the cylinder is at rest, the relative speed of the cylinder $U_r = U_w$, the vertical speed of the wall. The wall speed and the relative speed of rotation can be represented in dimensionless form as

$$\overline{U} = \frac{\mu U_w}{Mg}, \quad \Omega = \frac{R\omega}{U_w}, \tag{2}$$

respectively. This means that the distance between the cylinder and the wall establishes itself at $R\epsilon$, and we have

$$\epsilon = F(\mathrm{Bo}, h_R). \tag{3}$$

*Submerged cylinder.* As a first approximation, let us consider the case that the cylinder is surrounded entirely by the liquid, solved in Ref. [5], which in some sense corresponds to $h_R = \infty$. We expect the viscous forces to be dominated by the contribution from the narrow gap between the cylinder and the wall, a lubrication problem also treated in Ref. [5]. We adopt a Cartesian coordinate system $(x, y)$ with $\hat{\boldsymbol{x}}$ pointing vertically upwards (cf. Fig. 2) (so the acceleration due to

 

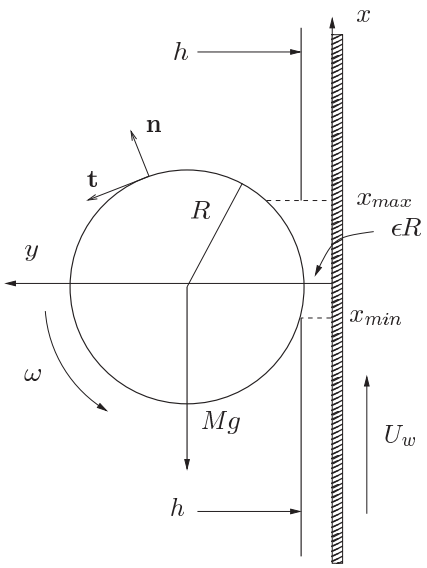


FIG. 2. Notation for theoretical model.

gravity $\boldsymbol{g} = -g\hat{\boldsymbol{x}}$), $\hat{\boldsymbol{y}}$ pointing toward the cylinder, and the origin defined as the nearest point on the wall to the cylinder.

Let the fluid velocity be $\boldsymbol{u} = u(x,y)\hat{\boldsymbol{x}} + v(x,y)\hat{\boldsymbol{y}}$ and the fluid pressure be $p(x,y)$; we confine ourselves to stationary situations in which the cylinder is a rest in the laboratory frame. Standard lubrication scalings motivate the following stretched coordinates:

$$X := \frac{x}{\sqrt{\epsilon}R}, \quad Y := \frac{y}{\epsilon R}, \tag{4}$$

and rescaled flow,

$$(u,v) := U_w(U, V\sqrt{\epsilon}), \tag{5}$$

and pressure fields,

$$p = \frac{\mu U_w}{\epsilon^{3/2}R}P. \tag{6}$$

The surface of the cylinder is then defined by

$$Y = H(X) := 1 + \tfrac{1}{2}X^2, \tag{7}$$

and the appropriate boundary conditions are

$$(U,V)|_{Y=0} = (1,0), \quad (U,V)|_{Y=H} = \Omega(1,X). \tag{8}$$

After these rescalings, the governing equations

$$\nabla p = \mu\nabla^2\boldsymbol{u} - g\hat{\boldsymbol{x}}, \qquad \nabla\cdot\boldsymbol{u} = 0 \tag{9}$$

become to leading order

$$\frac{\partial P}{\partial X} = \frac{\partial^2 U}{\partial Y^2}, \quad \frac{\partial P}{\partial Y} = 0, \tag{10}$$

$$\frac{\partial U}{\partial X} + \frac{\partial V}{\partial Y} = 0. \tag{11}$$

It follows that $P = P(X)$ and the equations are easily integrated to

$$U = \frac{1}{2}\frac{dP}{dX}(Y^2 - YH) + (\Omega - 1)\frac{Y}{H} + 1, \tag{12}$$

with solution

$$P = 3(\Omega+1)\left[\frac{X}{H} + \sqrt{2}\tan^{-1}\left(\frac{X}{\sqrt{2}}\right)\right] - 3Q\left[\frac{X}{H^2} + \frac{3X}{2H} + \frac{3}{\sqrt{2}}\tan^{-1}\left(\frac{X}{\sqrt{2}}\right)\right] + P_0, \tag{13}$$

where

$$Q = \int_0^H U\,dY \tag{14}$$

is the dimensionless flux in the frame of reference of the moving cylinder, which must be $X$-independent.

In the limit that the cylinder is covered completely, the boundary condition for $X \to \pm\infty$ is for the pressure to go to zero. This ensures that the pressure just outside of the gap remains finite in the limit $\epsilon \to 0$. This leads to the condition $Q = 2(\Omega+1)/3$, and a pressure distribution

$$P = -2(\Omega+1)\frac{X}{H^2},$$

which is *antisymmetric* about the cylinder. As a result, the force perpendicular to the wall vanishes. Therefore, the cylinder remains in an indifferent equilibrium position at a fixed distance $\epsilon R$ from the wall.

The total force on the cylinder parallel to the wall is

$$F_x := \int_{-\infty}^{\infty} \hat{\boldsymbol{x}}\cdot\boldsymbol{\sigma}\cdot\hat{\boldsymbol{n}}\Big|_{Y=H} dx - Mg = 4\pi\frac{\mu U_w}{\sqrt{2\epsilon}} - Mg. \tag{15}$$

Here, $\hat{\boldsymbol{n}}$ is the unit normal vector to the cylinder (cf. Fig. 2), and $\boldsymbol{\sigma}$ is the fluid stress tensor. Finally, the net torque around the center of the cylinder is

$$T := R\int_{-\infty}^{\infty} \hat{\boldsymbol{t}}\cdot\boldsymbol{\sigma}\cdot\hat{\boldsymbol{n}}\Big|_{Y=H} dx = 4\pi\frac{\mu\omega R^2}{\sqrt{2\epsilon}}. \tag{16}$$

The cylinder will not be rotating ($\omega = 0$) as the viscous torque counteracts any rotation [5]. From a balance between the viscous upward force and the weight of the cylinder, we have in dimensionless form

$$\overline{U} = \frac{\sqrt{2\epsilon}}{4\pi}. \tag{17}$$

Here, $\epsilon$ is arbitrary and cannot be determined by the dynamics as suggested by Eq. (3): there is no selection in the limit $h_R = \infty$. Instead, we must model the thin film present in the experiment, so that some input from the meniscus region is necessary. Another feature that is missing so far is that the cylinder is predicted not to rotate, if it is completely immersed in fluid.

*Thin film solution.* To remedy this situation, we introduce conditions at the upstream and downstream menisci, which account for the following experimental observations (see Fig. 2): (i) as the belt film approaches the cylinder, it meets the very thin film ($< 0.1$ mm) on the cylinder and both are sucked underneath the cylinder in a smooth fashion. Therefore, we assume that the position of the upstream meniscus is determined geometrically as the locus where the film meets the cylinder and will neglect the very thin film on the cylinder. (ii) On the other hand, as the fluid emerges downstream of the cylinder and separates into films on the cylinder and belt, fluid piles up to a larger scale: see Fig. 1(b). We assume that

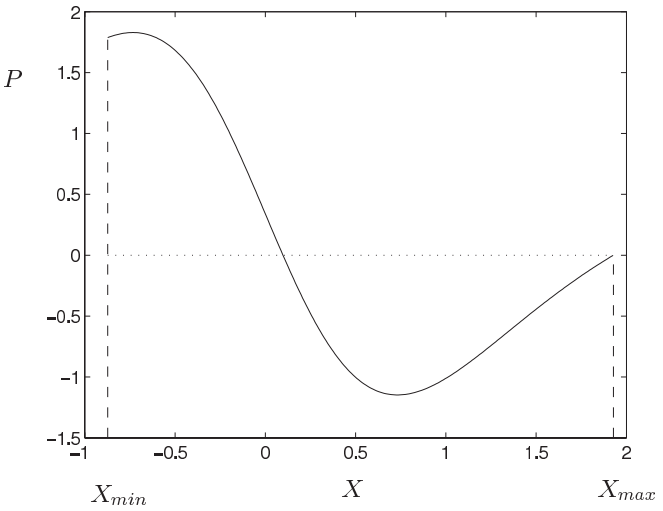


FIG. 3. A typical pressure distribution underneath the cylinder plotted over $[X_{\min}, X_{\max}]$, with $P(X_{\max}) = 0$ by construction.

surface tension does not play a leading role ($\mu U_w/\gamma \approx 7.4$ for a typical value of $U_w = 10$ mm/s) and, therefore, that the film pressure at the downstream meniscus is the ambient pressure, which we can take as zero. In terms of the rescaled variables, this leads to the two extra conditions:

$$X_{\min} = -\sqrt{2\,(h_R/\epsilon - 1)}, \tag{18}$$

$$P(X_{\max}) = 0. \tag{19}$$

To get a new solution, we are forced to assume a scaling in which the film only extends to *finite* values of $X_{\min}$ and $X_{\max}$; otherwise, we would fall back on the same pressure distribution as before. Now the constant $P_0$ in the pressure distribution Eq. (13) is determined by the downstream meniscus condition. The flux $Q$ follows from the condition that the mass influx from the film must equal the mass flux underneath the cylinder; it follows that $Q = h_R/\epsilon$. This leads to a new pressure distribution as shown in Fig. 3. The pressure is pushed up toward larger positive values in the upstream part, so as to make the integral over the pressure vanish. However, the asymmetric distribution of pressure allows for the torque to vanish at a finite frequency of rotation.

To determine the steady state of the system, we have to solve for the conditions of equilibrium $F_x = F_y = T = 0$, which can be written as

$$\frac{\overline{U}}{\sqrt{\epsilon}} \int_{X_{\min}}^{X_{\max}} X P \, dX = -1 \tag{20}$$

$$\int_{X_{\min}}^{X_{\max}} P \, dX = 0 \tag{21}$$

$$\int_{X_{\min}}^{X_{\max}} \left[ \frac{H}{2} P' + \frac{\Omega - 1}{H} \right] dX = 0. \tag{22}$$

For a given value of $\overline{U}/\sqrt{\epsilon}$, the set of Eqs. (22) is to be solved for $h_R/\epsilon$, $\Omega$, and $X_{\max}$. Thus, in particular, the nondimensional cylinder velocity is

$$\overline{U} = f\,(h_R/\epsilon)\,\sqrt{\epsilon}. \tag{23}$$

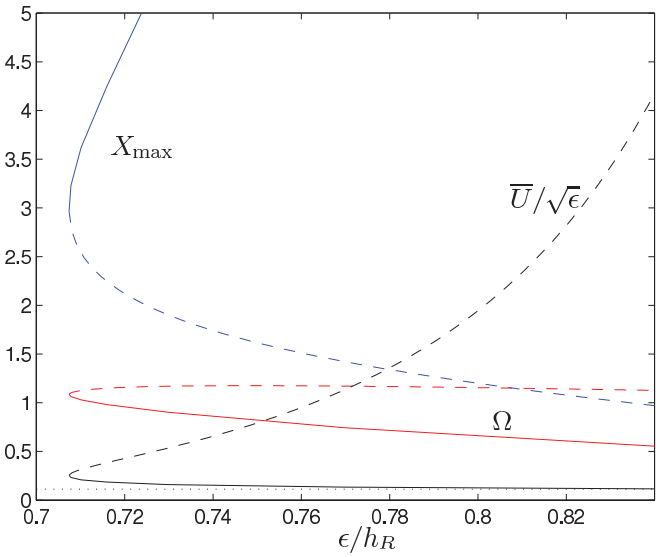


FIG. 4. (Color online) Predictions of the theoretical model as a function of $\epsilon/h_R$. All have an upper and lower branch with solid and dashed lines, indicating the two types of solution. The dotted line is Eq. (17) for the submerged cylinder.

The state of the system is determined by the value of $\epsilon/h_R$, which itself depends on the initial condition. The translation speed, relative rotation rate, and position $X_{\max}$ of the downstream meniscus are shown in Fig. 4. Note that there are two branches of solutions, of which only the lower one ($\Omega < 1$) describes the cylinder being driven by the belt. The upper solution ($\Omega > 1$) has the cylinder driving the belt, which seems unphysical and is, therefore, ignored hereafter. What is still missing is a mechanism for the selection of one particular value of $\epsilon/h_R$—the fractional size of the gap compared to the belt film thickness. In other words, within our thin film model,

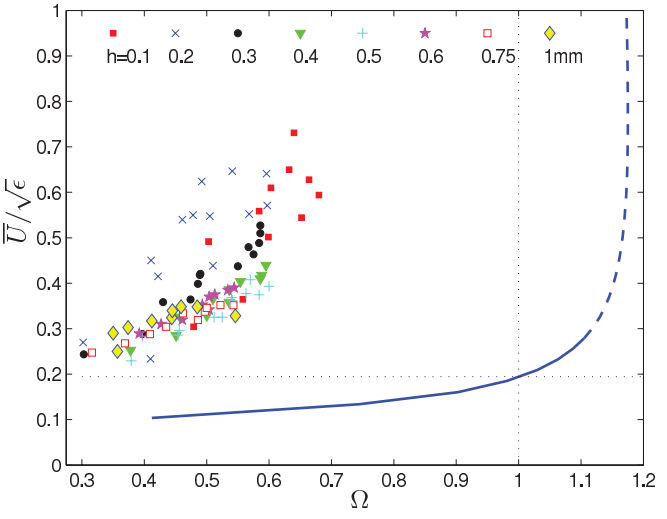


FIG. 5. (Color online) Comparison of theory with data on a plot of $\overline{U}/\sqrt{\epsilon}$ vs. $\Omega$. All the data has $\Omega < 1$, indicating that the lower (solid) $\Omega$ branch is the physically relevant one. Data are collected in sets defined by a specific belt film thickness (see key). Data with $h \leqslant 0.3$ mm may have been affected by belt roughness; note the improved collapse if these data are excluded.

the cylinder is in neutral equilibrium with respect to changes in the gap size.

*Comparison with data.* In Fig. 5, experimental data is plotted on a $\overline{U}/\sqrt{\epsilon}$ versus $\Omega$ plot, where now the theory is represented by a line parameterized by $\epsilon/h_R$. A choice has to be made for $\epsilon$ to generate an ordinate from the data, but fortunately $\epsilon$ is constrained to lie in the narrow range between the bifurcation point $\epsilon = 0.71\,h_R$ and $\epsilon = h_R$, for which the cylinder just touches the layer. For Fig. 5, we took the midpoint $\epsilon = 0.855\,h_R$, but results are rather insensitive to this particular choice. Figure 5 supports the conclusion that the simple lubrication model presented here captures the essence of the viscous force and torque balances. Reassuringly, the model admits solutions that have $\Omega < 1$ so that the belt drives the cylinder through the lubrication layer rather than the other (unphysical) way around (indicated by the "upper" dashed-line solution in Fig. 4). However, the belt speed is underestimated substantially.

Beyond the mismatch in the predicted and measured belt speeds, the model also requires both an unrealistically large value of $X_{\max}$ (i.e., one which exceeds $1/\sqrt{\epsilon}$ so extending downstream beyond the cylinder!) and a high pressure at $X_{\min}$ (see Fig. 3). Simple estimates of the pressure difference across a concave-outwards meniscus at this upstream location fail to accommodate this pressure difference by over an order of magnitude. Undoubtedly, a more complete 2D (numerical) treatment is needed of this interesting region instead of the simple-minded 1D lubrication presented here.

To summarize, we have presented a simple lubrication model of how a cylinder is able to balance against an upward-moving, viscous-film-covered belt. This model captures the gross features of the phenomenon but also has clear deficiencies. In particular, it seems necessary to include surface tension into a more realistic model, which explains the selection of a particular value of $\epsilon$. Taking the next step to generate a numerical solution seems the only way to unravel the intricacies of how the belt film and the cylinder film meet upstream and then subsequently separate downstream, a recurring issue in these types of flows [6–10].

*Acknowledgment.* We thank Andrew Hazel for valuable comments on the manuscript.

[1] S. J. Weinstein and K. J. Ruschak, Annu. Rev. Fluid Mech. **36**, 29 (2004).
[2] S. Kistler and E. P. M. Schweizer, *Liquid Film Coating* (Chapman and Hall, London, 1997).
[3] J. Bico, J. Ashmore-Chakrabarty, G. McKinley, and H. Stone, Phys. Fluids **21**, 082103 (2009).
[4] J. R. A. Pearson, J. Fluid Mech. **7**, 481 (1960).
[5] D. J. Jeffrey and Y. Onishi, Q. J. Mech. Appl. Math. **34**, 129 (1981).
[6] M. R. Hopkins, Br. J. Appl. Phys. **8**, 442 (1957).
[7] E. Pitts and J. Greiller, J. Fluid Mech. **11**, 33 (1961).
[8] K. J. Ruschak, J. Fluid Mech. **119**, 107 (1982).
[9] P. H. Gaskell, G. E. Innes, and M. D. Savage, J. Fluid Mech. **355**, 17 (1998).
[10] B. R. Duffy and S. K. Wilson, J. Fluid Mech. **394**, 29 (1999).